JACC: CARDIOONCOLOGY VOL. 6, NO. 1, 2024

ORIGINAL RESEARCH

Heart Failure Post-Myocardial Infarction Promotes Mammary Tumor Growth Through the NGF-TRKA Pathway

Tetsuya Tani, MD,[a] Masayoshi Oikawa, MD, PhD,[a] Tomofumi Misaka, MD, PhD,[a,b] Takafumi Ishida, MD, PhD,[a] Yasuchika Takeishi, MD, PhD[a]

ABSTRACT

BACKGROUND Epidemiological investigations suggest that patients with heart failure have a higher incidence of cancer; however, the causal role of cardiac disease on cancer progression remains unclear.

OBJECTIVES This study aimed to investigate the impact and underlying mechanisms of myocardial infarction (MI)–induced heart failure on tumor cell growth.

METHODS We generated a syngeneic mouse model by implanting mammary tumor–derived 4T1 cells into BALB/c mice with MI resulting from ligation of the left anterior descending artery.

RESULTS Mice with MI exhibited increased tumor volume, tumor weight, and Ki67-positive proliferative cells in the tumor tissue compared with the sham-operated mice. Furthermore, RNA sequencing analysis in the tumor tissue revealed significant enrichment of pathways related to tumor progression, particularly the PI3K-AKT pathway in the MI mice. Upregulation of tropomyosin receptor kinase A (TRKA) phosphorylation, an upstream regulator of PI3K-AKT signaling, was observed in the tumor tissue of the MI mice. We also observed elevated levels of circulating nerve growth factor (NGF), a ligand of TRKA, and increased NGF expressions in the myocardium after MI. In in vitro experiments, NGF stimulation led to increased cell proliferation, as well as phosphorylation of TRKA and AKT. Notably, inhibition of TRKA by small interfering RNA or the chemical inhibitor GW441756 effectively blocked these effects. Administration of GW441756 resulted in the suppression of tumor volume and cell proliferation in the MI mice.

CONCLUSIONS Our study demonstrates that MI promotes mammary tumor growth through the NGF-TRKA pathway. Consequently, inhibiting TRKA could represent a therapeutic strategy for breast cancer patients concurrently experiencing heart failure after MI. (J Am Coll Cardiol CardioOnc 2024;6:55-66) © 2024 The Authors. Published by Elsevier on behalf of the American College of Cardiology Foundation. This is an open access article under the CC BY-NC-ND license (http://creativecommons.org/licenses/by-nc-nd/4.0/).

From the [a]Department of Cardiovascular Medicine, Fukushima Medical University, Fukushima, Japan; and the [b]Department of Community Cardiovascular Medicine, Fukushima Medical University, Fukushima, Japan.
The authors attest they are in compliance with human studies committees and animal welfare regulations of the authors' institutions and Food and Drug Administration guidelines, including patient consent where appropriate. For more information, visit the Author Center.

Manuscript received June 16, 2023; revised manuscript received October 16, 2023, accepted October 17, 2023.

ISSN 2666-0873 https://doi.org/10.1016/j.jaccao.2023.10.002

ABBREVIATIONS AND ACRONYMS

ANOVA = analysis of variance

DMSO = dimethyl sulfoxide

MI = myocardial infarction

NGF = nerve growth factor

siRNA = small interfering RNA

TRKA = tropomyosin receptor kinase A

Despite advances in medical therapies, mortality rates from cardiovascular disease and cancer remain high.[1,2] Both cardiovascular disease and cancer share common risk factors, including diabetes, smoking, obesity, and inflammation.[3] Recent epidemiological studies have revealed a higher incidence of cancer in patients with heart failure compared with the general population[4] and have associated the presence of heart failure with an increased risk of future cancer incidence.[5] In addition, there is a rising prevalence of cancer patients with comorbid myocardial infarction (MI)[6] who face higher risks of mortality due to cancer progression and subsequent cardiovascular events,[6] including recurrent MI and heart failure. Notably, ischemic heart disease is a major cause of heart failure[7]; patients who experience heart failure after MI are at a higher risk of developing cancer compared with those without heart failure.[8] Although the link between MI and cancer is evident, the exact mechanisms by which cardiac disease affects cancer development are not yet fully understood. Consequently, investigating potential therapeutic strategies has become crucial to improve patient outcomes,[9] leading to the emergence of a new field called cardio-oncology, which focuses on studying the association between cardiac disease and cancer.[10]

Neurohumoral factors play essential roles in the development of cardiac remodeling and heart failure,[11,12] and several neurohumoral factors are known as critical molecules for activating intracellular signaling pathways of cancer cells, contributing to the progression of cancer.[13] Among these factors, nerve growth factor (NGF) has been identified as a promoter of cardiac hyperinnervation under pathological cardiac conditions such as MI and heart failure.[14] Tropomyosin receptor kinase A (TRKA), a specific receptor of NGF, is expressed on the cell membrane of breast cancer,[15,16] and it has been reported that overexpression of TRKA enhances breast cancer growth through the PI3K/AKT and MAPK/ERK signaling pathways.[15]

Cancer can develop through complex mechanisms, including evasion of growth suppressors, avoiding immune destruction, and sustaining proliferative signaling.[13] The PI3K/AKT signaling pathway plays an essential role in the process of sustained cell proliferation in response to extracellular signals, including humoral and growth factors.[17] However, it remains unclear whether the upregulation of NGF induced by MI could play a causative role in cancer development dependent on the TRKA receptor. Here, we aimed to investigate the causal role of MI on cancer progression, providing evidence that MI leads to tumor cell growth through the activation of the NGF-TRKA signaling pathway.

METHODS

A detailed description of the methods is provided in the Supplemental Methods.

MI IN MICE. Female mice with a BALB/c background, 8 to 12 weeks of age, were used for clinical scenarios replicating mammary tumors. These mice were subjected to either MI or sham surgeries, following the procedures as previously reported.[18,19] An intraperitoneal injection was administered to anesthetize the mice. During the operation, the mice underwent endotracheal intubation and ventilation. Subsequently, a left anterior thoracotomy was performed, exposing the heart, and the occlusion of the left anterior descending artery was executed.

ECHOCARDIOGRAPHY. Transthoracic echocardiography was performed, and the heart was observed in the short axis view near the papillary muscles in B-mode images.[20]

TRANSFECTION WITH SMALL INTERFERING RNA. To carry out the transfection, 4T1 cells were transfected with either scrambled negative control small interfering RNA (siRNA) or TRKA-specific siRNA.

SYNGENEIC MOUSE MODEL AND ASSESSMENT OF TUMOR GROWTH. Female BALB/c mice were anesthetized by intraperitoneal injection 2 weeks after MI or sham surgery. A total of 1×10^4 4T1 cells were orthotopically injected into the right fourth mammary fat pad of the mice.[21] Tumor volume was then measured using a digital caliper.[21] At the end of the study, mice were euthanized by cervical dislocation. The group allocation of the sham- or MI-operated mice was blinded during the tumor implantation process. Each experiment for tumor cell implantation was independently conducted 3 times.

HISTOLOGICAL ANALYSIS, IMMUNOFLUORESCENCE, AND IMAGE ANALYSIS. The paraffin-embedded section of the heart was stained with Elastica-Masson for histological analysis. For immunohistochemistry, paraffin sections of the tumor were subjected to reaction with an anti-Ki67 antibody.[22] Immunofluorescence was conducted on paraffin sections of both the tumor and cells using anti-Ki67 antibody.[22]

ENZYME-LINKED IMMUNOSORBENT ASSAY. The serum NGF concentrations in the peripheral blood

were measured using enzyme-linked immunosorbent assay.

RNA ISOLATION, RNA SEQUENCING, AND REVERSE-TRANSCRIPTION QUANTITATIVE POLYMERASE CHAIN REACTION. Total RNA was isolated from the implanted tumor tissues or the heart and subsequently purified. For RNA sequencing, gene expression was computed based on the reads, analyzing differentially expressed genes and gene ontology. For reverse-transcription quantitative polymerase chain reaction, complementary DNA was synthesized.

WESTERN BLOT ANALYSIS. Proteins were isolated from frozen mouse tumors, heart samples, or cultured cells. Aliquots of proteins were subjected to sodium dodecyl sulfate-polyacrylamide gel electrophoresis, transferred onto nitrocellulose membranes, and probed with the antibodies.[22]

CELL PROLIFERATION ASSAY. 4T1 cell proliferation was determined using a colorimetric MTS assay.[23]

ADMINISTRATION OF A TRKA INHIBITOR IN MICE. The TRKA inhibitor, GW441756, dissolved in dimethyl sulfoxide (DMSO), was administered to the MI- or sham-operated mice at a dose of 10 mg/kg via an intraperitoneal injection twice a week for 3 weeks.[24] Throughout the 4T1 implantation in both the MI- and sham-operated mice, as well as the intraperitoneal injection of GW441756 or DMSO, all procedures were carried out in a blinded manner. Each experiment for tumor cell implantation was independently conducted 4 times.

ASSESSMENT OF METASTASIS. For the assessment of metastasis, lung and the liver tissues were collected 3 weeks after 4T1 cell implantation. The paraffin-embedded tissue sections (3 μm) were stained with hematoxylin and eosin. Metastasis was assessed using ImageJ software 1.53a version (National Institutes of Health).[25,26]

STATISTICAL ANALYSIS. All data are expressed as the mean ± SEM. The Shapiro-Wilk test was used to assess normality. The unpaired Student's *t* test was performed to compare values between 2 groups. The PossionDis method was employed to obtain the false discovery rates in RNA sequencing analysis. False discovery rate values, along with adjusted *P* values, were used to generate the volcano plot, and Q values were used for the Kyoto Encyclopedia of Genes and Genomes pathways. Two-way analysis of variance (ANOVA) followed by Tukey's post hoc test for multiple pairwise comparisons were applied when 4 groups were evaluated. A 1-way repeated-measures ANOVA with Bonferroni's multiple comparisons test were applied for time and treatment comparisons in 2 groups. Two-way repeated-measures ANOVA with Tukey's multiple comparisons test were applied for times and treatment comparisons in 4 groups. A *P* value of <0.05 was considered statistically significant.

ETHICAL APPROVAL. All animal studies were reviewed and approved by the Fukushima Medical University Animal Research Committee (approval number 2022050). The protocols complied with relevant ethical regulations. All experiments followed the guidelines in the Guide for the Use and Care of Laboratory Animals from the Institute for Laboratory Animal Research. All efforts were made to minimize the suffering of the animals.

RESULTS

MI-INDUCED HEART FAILURE ACCELERATES MAMMARY TUMOR GROWTH IN MICE. To evaluate the causal relationship between MI-induced heart failure and tumor growth, we employed a syngeneic mouse model to replicate clinical scenarios involving tumor comorbidity with heart failure after MI. First, MI was induced by ligating the left anterior descending artery, resulting in a broad infarct area, functional abnormality, and increased lung weight, suggestive of pulmonary congestion with heart failure at 5 weeks after surgery (Supplemental Figure 1, Supplemental Table 1). Two weeks after the MI operation, 4T1 cell lines were implanted into the right fourth mammary fat pad of the mice (**Figure 1A**). Our findings revealed a gradual increase in tumor volume of the 4T1 cells in both sham- and MI-operated mice. Of note, the tumor volume was significantly greater in the MI-operated mice compared with the sham-operated control mice at both 2 and 3 weeks after tumor cell implantation (**Figure 1B**). At 3 weeks, tumor volume and tumor weight were significantly higher in the MI-operated mice compared with the sham-operated mice (**Figure 1C**). Furthermore, immunohistochemical analysis showed a significant increase in the percentage of Ki67-positive cells in the MI-operated mice compared with the sham-operated mice (**Figure 1D**). The survival rate after 4T1 cell implantation was significantly lower in the MI-operated mice than in the sham-operated mice (Supplemental Figure 2). Left ventricular ejection fraction or infarct area post-MI did not correlate with the size of the tumor (Supplemental Figure 3). To explore the involvement of MI in metastasis, we evaluated lung and liver metastasis[27] and found that the extent of the metastasis did not differ between the 2 groups (Supplemental Figure 4).

FIGURE 1 MI Accelerates Mammary Tumor Growth in Mice

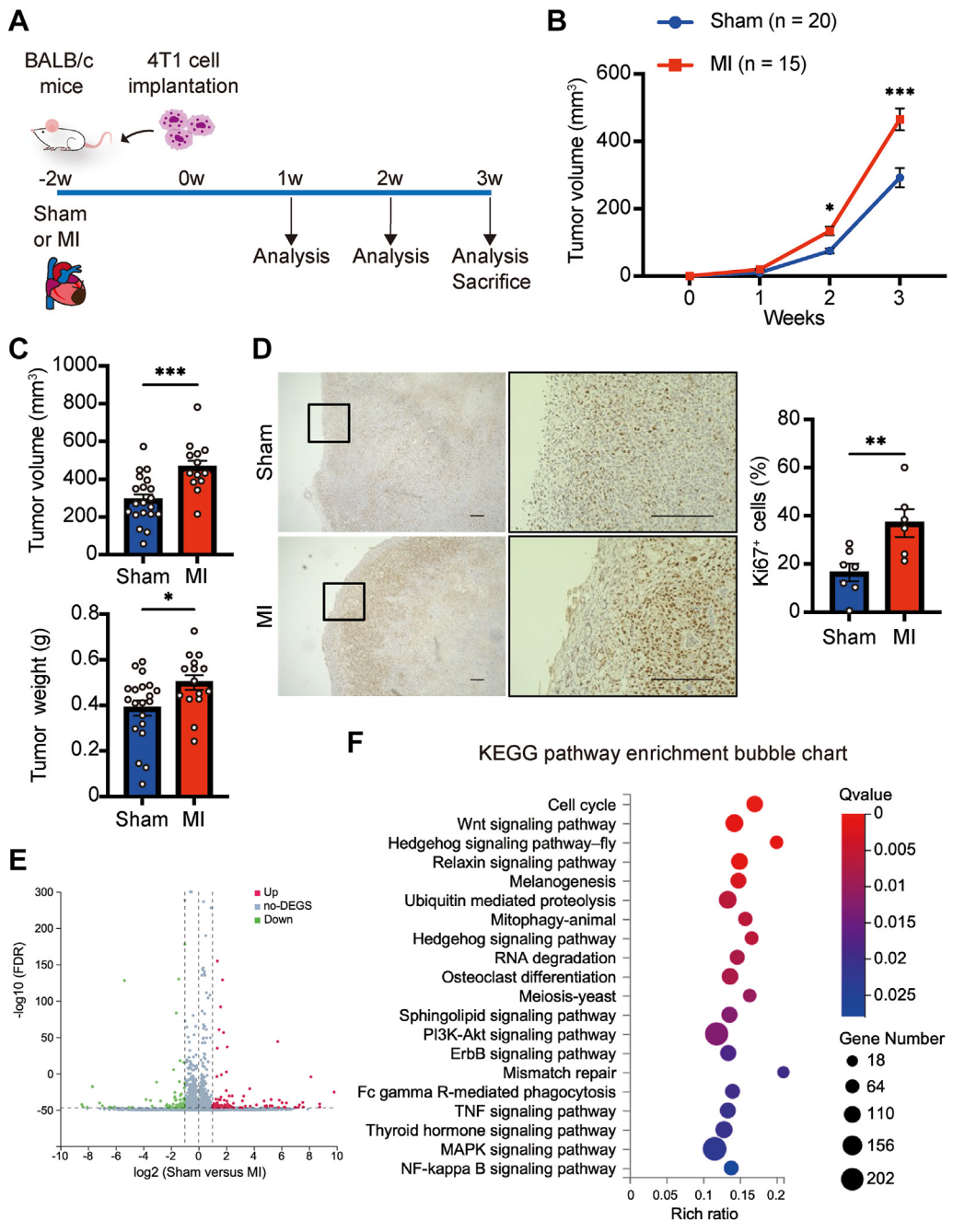

(A) The experimental setup for the syngeneic mouse model mimicking tumor comorbidity with myocardial infarction (MI). Ligation to the left ascending coronary artery induced MI or sham surgery. Implantation of mammary tumor-derived 4T1 cells occurred 2 weeks after the surgeries in female BALB/c mice. (B) Tumor growth over a 3-week period following 4T1 cell implantation. (C) Quantification of tumor volume and tumor weight 3 weeks after 4T1 cell implantation (sham = 20, MI = 15). (D) Representative images of tumor tissues immunostained with an anti-Ki67 antibody. Scale bars: 200 μm. The ratio of Ki67-positive cells is presented in the graph (right) (sham = 7, MI = 6). (E) Volcano plot of RNA sequence depicting differentially expressed genes in tumor tissues in MI-operated mice. Red and green dots represent upregulated and downregulated genes, respectively. Volcano plots depict mean log2 fold change against the −log10 false discovery rate (FDR)-adjusted *P* values for all expressed genes. (F) Kyoto Encyclopedia of Genes and Genomes (KEGG) analyses of RNA sequencing from tumor tissues, with bubble plot demonstrating all KEGG enrichment pathways, Q values, and rich ratio in MI-operated mice compared with sham-operated mice. Circle size depicts the number of genes annotated to each KEGG pathway. Data are presented as mean ± SEM. *$P < 0.05$, **$P < 0.01$, and ***$P < 0.001$, determined by a 1-way repeated-measures analysis of variance with (B) Bonferroni's multiple comparisons test or (C, D) 2-tailed unpaired Student's *t* test. DEG = differentially expression gene.

Next, we performed RNA sequencing to assess the mechanistic relevance of accelerated tumor cell growth in MI. Comparative analysis of the gene expression levels in the tumor tissues of the MI- and sham-operated mice showed 4,694 upregulated genes and 4,103 downregulated genes in the tumors of the MI mice compared with those of the sham mice (**Figure 1E**). Pathway enrichment analysis using Kyoto Encyclopedia of Genes and Genomes revealed significant enrichment of several crucial pathways associated with tumor progression, including the cell cycle and PI3K-AKT pathway, in the MI-operated mice (**Figure 1F**).

INVOLVEMENT OF CIRCULATING NERVE GROWTH FACTOR IN THE TRKA RECEPTOR–RELATED SIGNALING OF THE TUMOR TISSUES. Given the potential association between humoral factors and tumor development,[13] we sought to investigate the relationship between circulating ligands altered after MI and the receptors expressed on the tumor cells. Based on our findings from RNA sequencing, which indicated the activation of the PI3K-AKT pathway in the tumor tissues of the MI-operated mice, we investigated the secreting factors that play a pivotal role in regulating this pathway. Specifically, because the neurotrophin family is recognized as central upstream regulators of the PI3K-AKT pathway,[28] we focused on neurotrophins such as NGF, which exhibits the greatest affinity to TRKA, and brain-derived neurotrophic factor, the ligand of TRKB. We found a significant increase in serum concentration of NGF in peripheral blood at both 2 and 5 weeks after MI (**Figures 2A and 2B**), whereas circulating brain-derived neurotrophic factor levels in peripheral blood remained unchanged at 2 and 5 weeks after MI (Supplemental Figure 5). The messenger RNA expression level of *Ngf* increased in the myocardium in the border area of the infarct zone 3 days after MI, compared with the sham-operated myocardium (**Figure 2C**). However, it did not change in the remote area of the infarct heart (**Figure 2D**). Likewise, NGF protein expression was elevated in the myocardium in the border area of the infarction (**Figures 2E and 2F**). Neither the messenger RNA levels of *Trka* nor the levels of phosphorylated TRKA in the heart exhibited significant induction in response to MI in the absence of 4T1 cell implantation (Supplemental Figure 6). In the tumor tissues, phosphorylation levels of TRKA, AKT, and ERK were significantly upregulated in the MI mice compared with the sham mice (**Figure 2G**, Supplemental Figure 7). Although it has been reported that immune reprogramming by MI is involved in tumor growth[21] and NGF-TRKA plays a potential role in immune response,[29] the numbers of infiltrating inflammatory cells such as M2 macrophages or expression levels of inflammatory cytokines such as *Il1b* in the tumor tissue did not differ between the sham mice and MI mice (Supplemental Figure 8). These data suggest that MI led to elevated expressions of NGF in the myocardium as well as NGF in the circulation, subsequently resulting in the phosphorylation of TRKA in the tumor tissue, which may play a role in accelerating tumor growth in mice with MI-induced heart failure.

THE NGF-TRKA PATHWAY IS VITAL FOR ACCELERATED PROLIFERATION IN 4T1 CELLS. Next, we explored the impact of the NGF-TRKA pathway on cell growth in cultured 4T1 cells. Stimulation with NGF in 4T1 cells led to a clear induction of phosphorylation levels of TRKA, AKT, and ERK (**Figure 3A**, Supplemental Figure 9). Cell proliferation was promoted in response to NGF stimulation, as assessed by immunostaining for Ki67 and MTS cell viability assay (**Figures 3B and 3C**). In contrast, when TRKA was knocked down in the cells using siRNA, the ratio of Ki67-positive cells did not increase upon NGF stimulation (**Figures 3D and 3E**). Furthermore, although phosphorylation levels of AKT were significantly upregulated in control cells after NGF treatment, AKT phosphorylation was significantly suppressed in TRKA-knockdown cells (**Figure 3F**). We next investigated the effects of the TRKA inhibitor GW441756 in cell proliferation and found that GW441756 inhibited the NGF-induced increases in the ratio of Ki67-positive proliferating cells as well as in the total number of cells (**Figures 3G and 3H**). Phosphorylation levels of AKT were upregulated in the control cells after NGF stimulation, whereas AKT phosphorylation was significantly suppressed by GW441756 (**Figure 3I**). These results indicate that the NGF-TRKA pathway plays a vital role in the proliferation of 4T1 cells.

INHIBITION OF TRKA SUPPRESSES THE TUMOR GROWTH INDUCED BY MI IN MICE. To clarify the effects of inhibition of TRKA on tumor progression induced by MI in mice, we treated the mice implanted with 4T1 cells using GW441756 (**Figure 4A**). We found that administration of GW441756 significantly reduced tumor volume in the MI mice compared with the DMSO-treated MI mice (**Figures 4B and 4C**). Accordingly, tumor weight was significantly lower in the GW441756-treated MI mice than in the DMSO-treated MI mice (Supplemental Figure 10). GW441756 did not affect the left ventricular function or the extent of the infarct size of the left ventricle

FIGURE 2 Changes in the NGF-TRKA Axis After MI in Mice

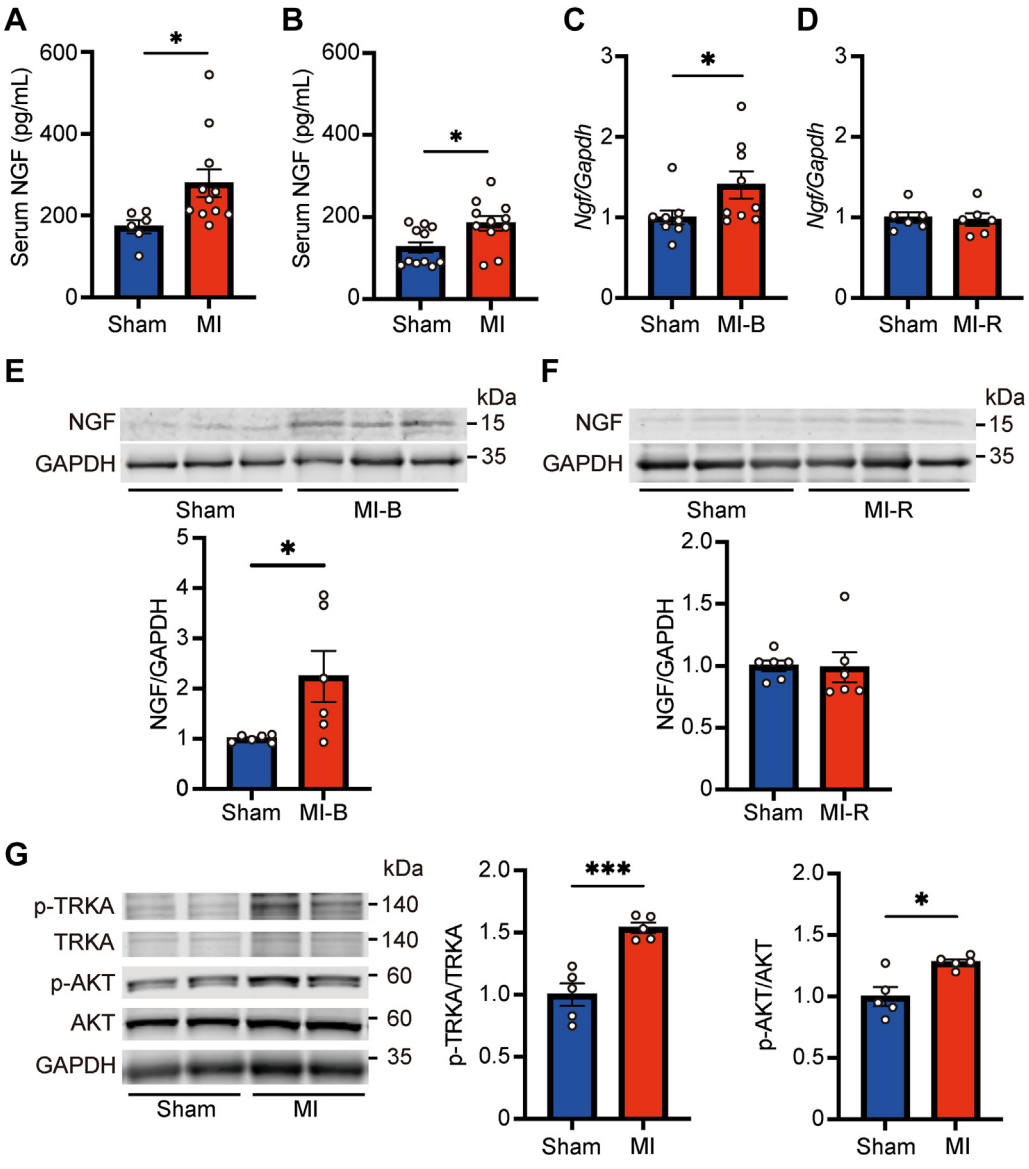

(A, B) Serum nerve growth factor (NGF) concentration at (A) 2 weeks and (B) 5 weeks after sham or myocardial infarction (MI) surgery (A: sham = 6, MI = 11; B: sham = 11, MI = 11). (C, D) Messenger RNA (mRNA) expressions of *Ngf* in the heart at the border area (MI -B) (n = 9 in each, C) and the remote area (MI -R) (n = 6 in each, D) 3 days after MI. (E, F) NGF protein expressions in the heart at (E) the border area (MI-B) and (F) the remote area (MI-R) 3 days after MI. The densitometric analyses are shown in the graphs (n = 6 in each). (G) Tropomyosin receptor kinase A (TRKA) and AKT phosphorylation in tumor tissues of the sham-operated and MI-operated mice. The ratios of phosphorylated TRKA (p-TRKA) to total TRKA and phosphorylated AKT (p-AKT) to total AKT are quantified, and the densitometric analyses are shown in the graphs (n = 5 in each). GAPDH was used as the loading control. Data are presented as mean ± SEM. *$P < 0.05$ and ***$P < 0.001$, determined by 2-tailed unpaired Student's *t* test.

(Supplemental Figure 11, Supplemental Table 2), nor did it alter detectable levels of TRKA phosphorylation in the heart (Supplemental Figure 12). The percentage of Ki67-positive cells in the tumor tissue was significantly decreased in the GW441756-treated MI mice compared with the DMSO-treated MI mice (**Figure 4D**). Additionally, phosphorylation levels of TRKA and AKT in the tumor tissues of the GW441756-treated MI mice were downregulated compared with those of the DMSO-treated MI mice (**Figure 4E**).

FIGURE 3 Essential Role of NGF/TRKA Pathway in Cell Proliferation in 4T1 Cells

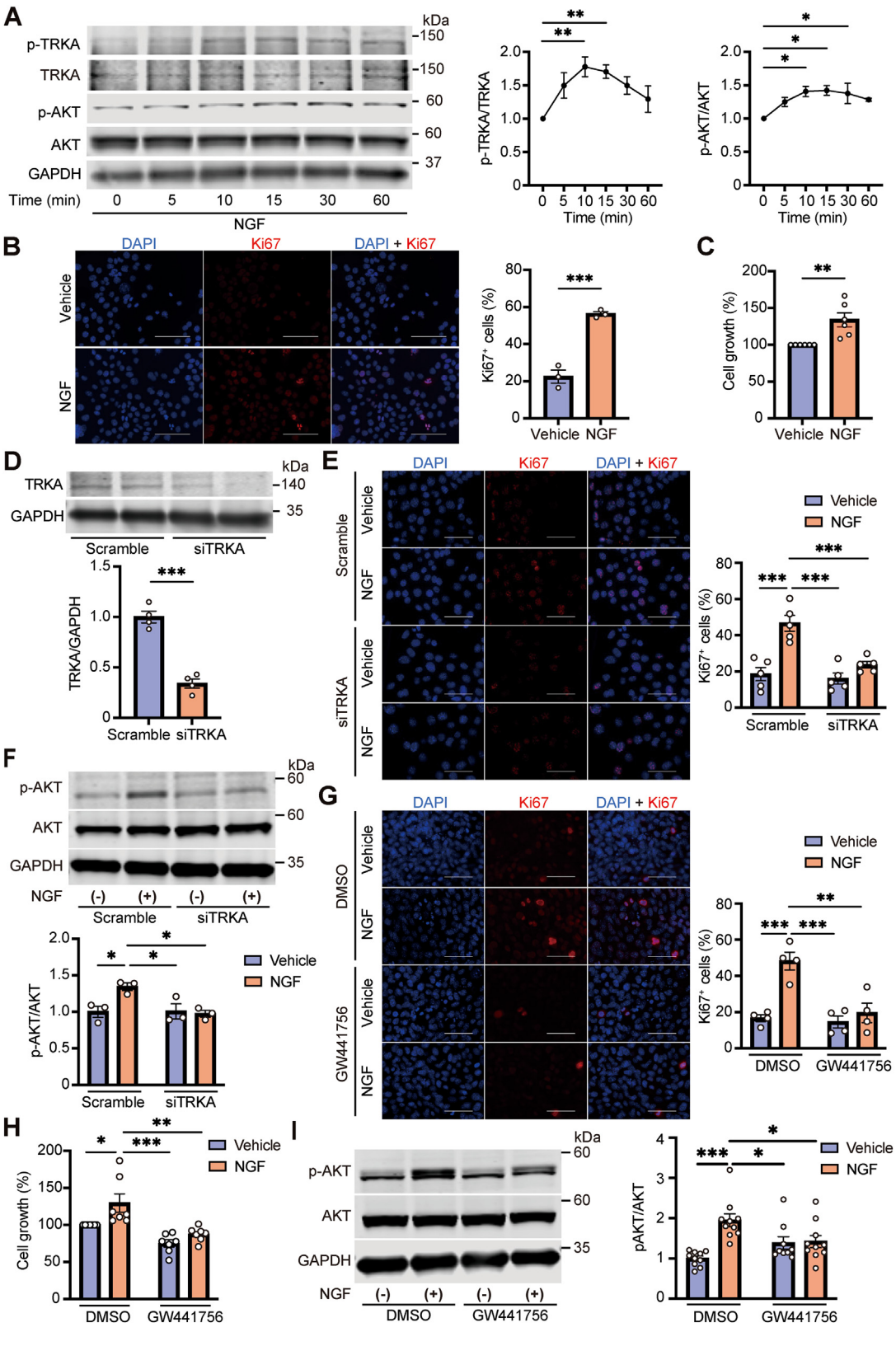

Continued on the next page

The administration of GW441756 did not yield significant alterations in either the quantities of immune cell infiltration or the expression levels of inflammatory cytokines in the tumor tissue (Supplemental Figure 13). Taken together, these findings suggest that the NGF-TRKA pathway is involved in accelerated tumor cell growth induced by heart failure after MI.

DISCUSSION

The present study is the first to demonstrate that the presence of MI-induced heart failure promoted mammary tumor cell growth through the NGF-TRKA pathways. Our results suggest that the inhibition of TRKA signaling pathways may be a potential therapeutic target for patients with breast cancer after MI (**Central Illustration**).

Although the association between MI and cancer is supported by epidemiological findings, the presence of multiple comorbidities and confounding factors complicates the understanding of the causal relationship among cancer incidence, cancer development, and MI. In the present study, we used a syngeneic mouse model harboring MI to clarify the direct contribution of abnormalities in humoral factors resulting from MI to cancer progression. Our experimental design reflects the presence of cardiac dysfunction preceding the tumor occurrence, as we implanted tumor cells after MI, whereas a previous study conducted tumor cell implantation before MI surgery in mice.[21] Our approach provides clinical scenarios that mimic the increased risk of future cancer incidence observed in patients with heart failure.[4,8] Although we used female BALB/c mice to establish the syngeneic mouse model to share the same genetic background of the 4T1 tumor cell line, BALB/c mice have been reported to exhibit a higher survival rate compared with other mouse strains,[30] indicating that the use of BALB/c mice is a suitable model for heart failure after MI.

NGF was initially discovered as a neurotrophic protein essential for the development of sympathetic and sensory afferent neurons,[31] and its disruption of NGF led to a lethal phenotype.[32] In the MI-diseased heart, we observed a persistent elevation of serum NGF concentrations, along with upregulation of NGF in the border area at the transcriptional and protein levels, even in the absence of tumors. Although NGF produced by cardiomyocytes is reported to play a cardioprotective role by preventing pathological ventricular remodeling,[33,34] excessive secretion of NGF into the bloodstream from the myocardium may promote mammary cancer growth when present at pathological levels.

The PI3K pathway is one of the most commonly activated signaling pathways in human cancer, typically activated by receptor tyrosine kinases such as TRKA.[35] Downstream of the NGF-TRKA pathway, the PI3K pathway holds significance in tumor initiation and progression, and targeting receptor tyrosine kinases upstream has shown to be effective.[35] In addition, the suppression of breast cancer development in mice through the inhibition of NGF

FIGURE 3 Continued

(A) Effects of the NGF ligand on the phosphorylation of TRKA and AKT in cultured 4T1 cells. The cells were stimulated with NGF (100 ng/mL) for the indicated time, and cell lysates were subjected to Western blot analysis. The ratios of p-TRKA to total TRKA (n = 5 in each) and p-AKT to total AKT were quantified. Densitometric analyses results are shown in the graphs (n = 3 in each). (B) Impact of NGF on 4T1 cell proliferation. The cells were stimulated with NGF for 24 hours and stained with an anti-Ki67 antibody and DAPI. Scale bars: 50 μm. Quantitative analysis of Ki67-positive cells (n = 3 in each). (C) Cell numbers were determined by MTS cell proliferation assay and expressed as a relative ratio over the vehicle group (n = 6 in each). (D) 4T1 cells were transfected with TRKA-specific small interfering RNA (siTRKA) or nontargeting control small interfering RNA (scramble) with 120 nM for 72 hours. TRKA expression was assessed by immunoblotting, and densitometric analysis is shown in the graph (n = 4 in each). (E) Role of TRKA in NGF ligand-associated cell proliferation. Transfected cells were incubated with NGF (100 ng/mL) or vehicle for 24 hours, and cells were fixed and immunostained with an anti-Ki67 antibody and DAPI. Representative images are shown in the left panels. Scale bars: 50 μm. Quantification of the ratios of Ki67-positive cells is shown in the right graph (n = 5 in each). (F) The levels of AKT phosphorylation in the TRKA-knockdown 4T1 cells in the presence of NGF for 15 minutes. Densitometric analyses are shown in the graph (n = 3 in each). (G) Effects of a chemical inhibitor of TRKA GW441756 on cell growth. 4T1 cells were incubated with GW441756 (1.25 μmol/L) or dimethyl sulfoxide (DMSO) for 24 h before NGF administration. A total of 24 hours after NGF stimulation, the cells were fixed and immunostained with an anti-Ki67 antibody and DAPI. Representative images are shown in the left panels. Scale bars: 50 μm. Quantification of the ratios of Ki67-positive cells is shown in the right graph (n = 4 in each). (H) Cellular viability was determined by MTS assay. The value in the vehicle group treated with NGF was set to 1 (n = 7 in each). (I) The levels of AKT phosphorylation in the 4T1 cells, which were incubated with GW441756 (1.25 μmol/L) or DMSO for 24 hours and then stimulated with NGF for 15 min. Densitometric analyses are shown in the graphs (n = 9-10). Data are presented as mean ± SEM. *$P < 0.05$, **$P < 0.01$, and ***$P < 0.001$, determined by (A) 1-way repeated measures analysis of variance with Bonferroni's multiple comparisons test, (B, C) 2-tailed unpaired Student's *t* test, or (E to I) 2-way analysis of variance with Tukey's multiple comparisons test. Abbreviations as in **Figure 2**.

FIGURE 4 Inhibition of TRKA Suppresses Tumor Progression in MI Mice

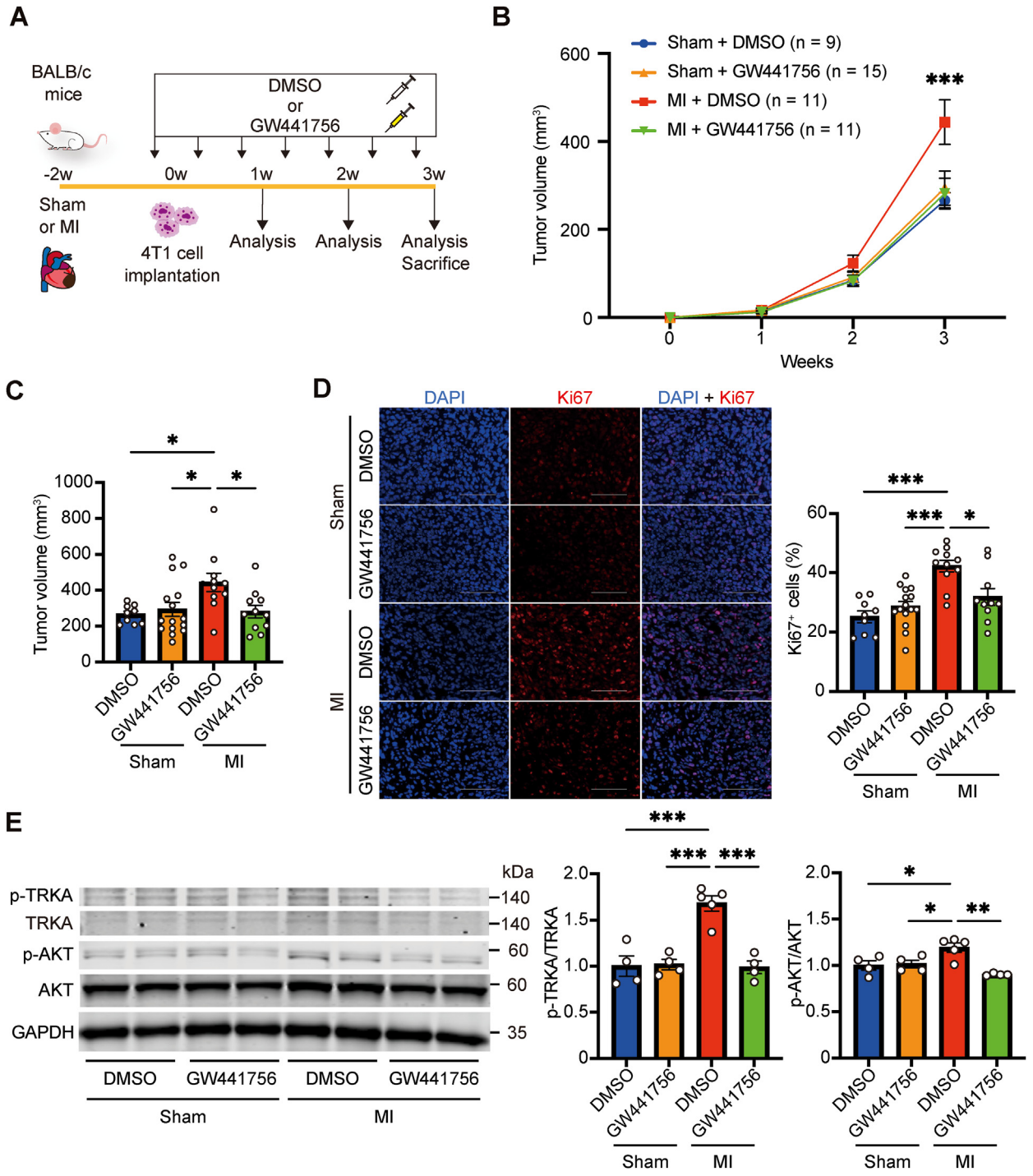

(A) Experimental protocol. Two weeks after sham or myocardial infarction (MI) operation, 4T1 cells were implanted into female BALB/c mice. Intraperitoneal injections of either dimethyl sulfoxide (DMSO) or GW441756, a TRKA inhibitor (10 mg/kg), were administered twice a week for 3 weeks. (B) Tumor growth over a 3-week period following cell implantation (sham + DMSO = 9, sham + GW441756 = 15, MI + DMSO = 11, MI + GW441756 = 11). (C) Quantification of tumor volume at 3 weeks after 4T1 cell implantation. (D) Tumor tissues were stained with an anti-Ki67 antibody and DAPI. Representative images and quantification of Ki67-positive cells are shown (n = 9-15). Scale bars: 100 μm. (E) The phosphorylation of TRKA and AKT in tumor tissues in the GW441756-treated mice. The ratios of p-TRKA to total TRKA and p-AKT to total AKT are quantified, and the densitometric analyses are shown in the graphs (n = 4-5). Data are presented as mean ± SEM. *$P < 0.05$, **$P < 0.01$, and ***$P < 0.001$, determined by (B) 2-way repeated-measures analysis of variance with Tukey's multiple comparisons test or (C to E) 2-way analysis of variance with Tukey's multiple comparisons test. Abbreviations as in Figures 2 and 3.

CENTRAL ILLUSTRATION **Impact of NGF-TRKA Pathway in Tumor Progression After MI**

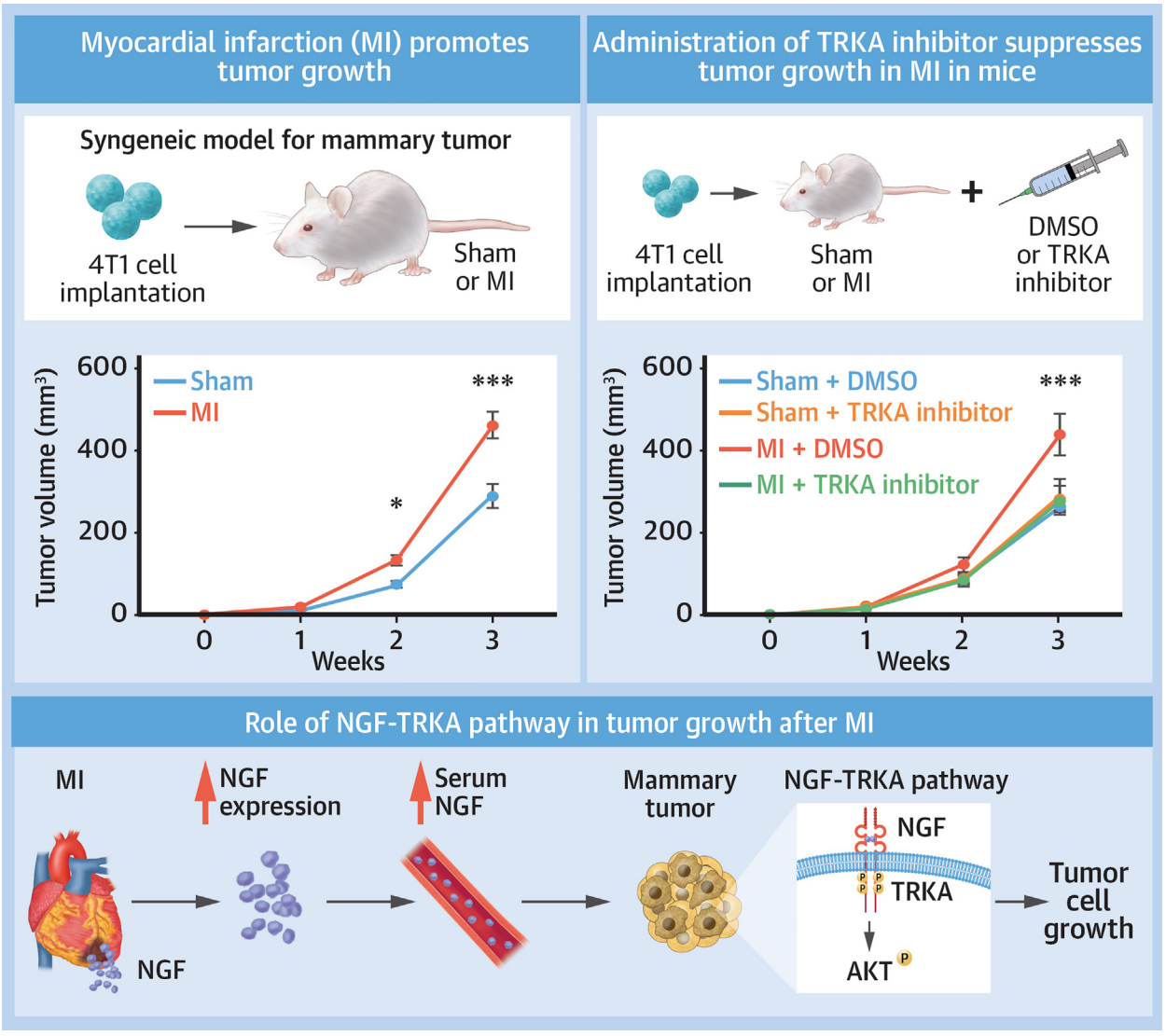

Tani T, et al. J Am Coll Cardiol CardioOnc. 2024;6(1):55-66.

A syngeneic mouse model was established by implanting mammary tumor-derived 4T1 cells into a BALB/c mouse with myocardial infarction (MI). Tumor volume was increased in MI mice compared with sham-operated mice. Phosphorylation of tropomyosin receptor kinase A (TRKA), upstream of PI3K-AKT signaling, in tumor tissue was upregulated in MI mice. Circulating levels of nerve growth factor (NGF), a TRKA ligand, and NGF expressions in the myocardium were elevated after MI. Administration of a TRKA inhibitor, GW441756, suppressed tumor volume in the MI mice. Data are presented as mean ± SEM. $*P < 0.05$ and $***P < 0.001$, determined by a 1-way repeated-measures analysis of variance with Bonferroni's multiple comparisons test or a 2-way repeated-measures analysis of variance with Tukey's multiple comparisons test.

using anti-NGF antibody has been reported.[16] Although various upstream molecules contribute to the activation of the PI3K-AKT pathway, NGF assumes a prominent role among the regulatory factors in tumor progression in patients with MI-induced heart failure.

Several TRK inhibitors are currently under investigation for the specific treatment of patients with NTRK fusion-positive solid tumors.[36] Larotrectinib, a selective TRK inhibitor, has recently demonstrated efficacy in TRK fusion gene-positive cancers, including mammary analogue secretory carcinoma,

with an overall response rate of 75%.[37] Likewise, our data suggest that TRKA inhibition could have an antitumor effect in patients with cardiac disease by suppressing the NGF-TRKA pathway. Recent anticancer drugs primarily focus on genetic abnormalities within cancer itself as molecularly targeted drugs. In contrast, our results suggest that the TRKA inhibitor has the potential to target not only the genetic abnormalities within cancer, but also humoral factor-mediated cancer progression. Furthermore, the inhibition of TRKA did not affect the cardiac function or infarct size in the MI-operated mice. Therefore, targeting TRKA represents a promising therapeutic approach for treating mammary cancer growth in patients with concomitant cardiac conditions like heart failure and MI.

A prior study indicated that MI accelerates breast cancer growth through innate immune reprogramming.[21] In contrast, our investigation demonstrates that the quantities of immune cell infiltration or the expression levels of inflammatory cytokines in the tumor tissue were comparable between mice that underwent MI and those that underwent sham operations, as well as between DMSO-treated and TrkA inhibitor-treated MI mice. In our speculation, the different experimental protocols may be a possible reason for these discrepant results. Koelwyn et al[21] conducted tumor cell implantation before MI surgery in mice, whereas we transplanted the tumor cells after MI. The variation in the timing of MI induction and the tumor cell implantation might have changed the immune circumstances around tumor tissue, warranting further research.

Considering our study's findings that the presence of MI is unlikely to affect metastasis in mammary cancer, it appears that the NGF-TRKA pathway may play distinct roles in cancer cell growth compared with metastasis. Recent findings highlighting the substantial transformation of the genomic landscape during advanced tumorigenic stages and metastatic tumors suggest that primary tumor growth and metastatic cancer may not share common mechanistic insight.[38] Further investigation is needed to understand the precise mechanisms by which MI affects the metastasis process.

STUDY LIMITATIONS. First, the implantation of 4T1 cell was performed in the subacute phase of MI, potentially confounding the influence of hemodynamic effects on breast cancer development. Second, although other humoral factors responsive to the pathological condition resulting from MI might contribute to tumor progression, a comprehensive analysis of these factors was not performed in this study. Third, the significance of NGF and other humoral factors in tumor progression in patients with MI was not evaluated, necessitating further research. Finally, the bidirectional relationship of MI-induced cardiac dysfunction and tumor growth may contribute to cancer progression, and the specific underlying mechanism requires further elucidation.

CONCLUSIONS

MI promotes mammary tumor growth through the NGF-TRKA pathway, suggesting that the inhibition of TRKA could be a promising therapeutic target for breast cancer patients with comorbid heart failure after MI.

ACKNOWLEDGMENTS The authors appreciate Tomiko Miura, Tomoko Ogata, Chisato Kubo, and Yoshiko Fukuda for their excellent technical assistance. They also thank Amane Yasunaga and Wataru Kamimura for their experimental support. The Central Illustration was created with BioRender.com.

FUNDING SUPPORT AND AUTHOR DISCLOSURES

This work was supported by the Japan Society for the Promotion of Science KAKENHI grants 22K08190 to Dr Tani and 20K08493, 23K07537 to Dr Oikawa. The authors have reported that they have no relationships relevant to the contents of this paper to disclose.

ADDRESS FOR CORRESPONDENCE: Dr Masayoshi Oikawa, Department of Cardiovascular Medicine, Fukushima Medical University, 1 Hikarigaoka, Fukushima 960-1295, Japan. E-mail: moikawa@fmu.ac.jp.

PERSPECTIVES

COMPETENCY IN MEDICAL KNOWLEDGE: MI accelerates mammary cancer progression through activation of the NGF-TRKA pathway, and the inhibition with a TRKA inhibitor suppresses tumor progression.

TRANSLATIONAL OUTLOOK: The inhibition of the NGF-TRKA pathway may be a potential therapeutic target for patients with breast cancer with comorbid heart failure after MI.

REFERENCES

1. Timmis A, Vardas P, Townsend N, et al. European Society of Cardiology: cardiovascular disease statistics 2021. *Eur Heart J*. 2022;43:716–799.

2. Bray F, Laversanne M, Weiderpass E, Soerjomataram I. The ever-increasing importance of cancer as a leading cause of premature death worldwide. *Cancer*. 2021;127:3029–3030.

3. Koene RJ, Prizment AE, Blaes A, Konety SH. Shared risk factors in cardiovascular disease and cancer. *Circulation*. 2016;133:1104–1114.

4. Banke A, Schou M, Videbaek L, et al. Incidence of cancer in patients with chronic heart failure: a long-term follow-up study. *Eur J Heart Fail*. 2016;18:260–266.

5. Hasin T, Gerber Y, McNallan SM, et al. Patients with heart failure have an increased risk of incident cancer. *J Am Coll Cardiol*. 2013;62:881–886.

6. Velders MA, Hagstrom E, James SK. Temporal trends in the prevalence of cancer and its impact on outcome in patients with first myocardial infarction: a nationwide study. *J Am Heart Assoc*. 2020;9:e014383.

7. Savarese G, Becher PM, Lund LH, Seferovic P, Rosano GMC, Coats AJS. Global burden of heart failure: a comprehensive and updated review of epidemiology. *Cardiovasc Res*. 2023;118:3272–3287.

8. Hasin T, Gerber Y, Weston SA, et al. Heart failure after myocardial infarction is associated with increased risk of cancer. *J Am Coll Cardiol*. 2016;68:265–271.

9. Yoshihisa A, Ichijo Y, Watanabe K, et al. Prior history and incidence of cancer impacts on cardiac prognosis in hospitalized patients with heart failure. *Circ J*. 2019;83:1709–1717.

10. Riffo-Campos AL, Domingo J, Dura E. OncoCardioDB: a public and curated database of molecular information in onco-cardiology/cardio-oncology. *Database (Oxford)*. 2023:2023:baad029.

11. Lymperopoulos A, Rengo G, Gao E, Ebert SN, Dorn GW 2nd, Koch WJ. Reduction of sympathetic activity via adrenal-targeted GRK2 gene deletion attenuates heart failure progression and improves cardiac function after myocardial infarction. *J Biol Chem*. 2010;285:16378–16386.

12. Lymperopoulos A, Rengo G, Koch WJ. Adrenergic nervous system in heart failure: pathophysiology and therapy. *Circ Res*. 2013;113:739–753.

13. Hanahan D, Weinberg RA. Hallmarks of cancer: the next generation. *Cell*. 2011;144:646–674.

14. Zhou S, Chen LS, Miyauchi Y, et al. Mechanisms of cardiac nerve sprouting after myocardial infarction in dogs. *Circ Res*. 2004;95:76–83.

15. Lagadec C, Meignan S, Adriaenssens E, et al. TrkA overexpression enhances growth and metastasis of breast cancer cells. *Oncogene*. 2009;28:1960–1970.

16. Adriaenssens E, Vanhecke E, Saule P, et al. Nerve growth factor is a potential therapeutic target in breast cancer. *Cancer Res*. 2008;68:346–351.

17. Jiang BH, Liu LZ. PI3K/PTEN signaling in angiogenesis and tumorigenesis. *Adv Cancer Res*. 2009;102:19–65.

18. Oikawa M, Wu M, Lim S, et al. Cyclic nucleotide phosphodiesterase 3A1 protects the heart against ischemia-reperfusion injury. *J Mol Cell Cardiol*. 2013;64:11–19.

19. Gao XM, Dart AM, Dewar E, Jennings G, Du XJ. Serial echocardiographic assessment of left ventricular dimensions and function after myocardial infarction in mice. *Cardiovasc Res*. 2000;45:330–338.

20. Vinhas M, Araújo AC, Ribeiro S, Rosário LB, Belo JA. Transthoracic echocardiography reference values in juvenile and adult 129/Sv mice. *Cardiovasc Ultrasound*. 2013;11:12.

21. Koelwyn GJ, Newman AAC, Afonso MS, et al. Myocardial infarction accelerates breast cancer via innate immune reprogramming. *Nat Med*. 2020;26:1452–1458.

22. Kimishima Y, Misaka T, Yokokawa T, et al. Clonal hematopoiesis with JAK2V617F promotes pulmonary hypertension with ALK1 upregulation in lung neutrophils. *Nat Commun*. 2021;12:6177.

23. Chowdhury P, Lin GE, Liu K, Song Y, Lin FT, Lin WC. Targeting TopBP1 at a convergent point of multiple oncogenic pathways for cancer therapy. *Nat Commun*. 2014;5:5476.

24. Singh R, Karri D, Shen H, et al. TRAF4-mediated ubiquitination of NGF receptor TrkA regulates prostate cancer metastasis. *J Clin Invest*. 2018;128:3129–3143.

25. Wagenblast E, Soto M, Gutierrez-Angel S, et al. A model of breast cancer heterogeneity reveals vascular mimicry as a driver of metastasis. *Nature*. 2015;520:358–362.

26. Kappes L, Amer RL, Sommerlatte S, et al. Ambrisentan, an endothelin receptor type A-selective antagonist, inhibits cancer cell migration, invasion, and metastasis. *Sci Rep*. 2020;10:15931.

27. Lambert AW, Pattabiraman DR, Weinberg RA. Emerging biological principles of metastasis. *Cell*. 2017;168:670–691.

28. Meng L, Liu B, Ji R, Jiang X, Yan X, Xin Y. Targeting the BDNF/TrkB pathway for the treatment of tumors. *Oncol Lett*. 2019;17:2031–2039.

29. Minnone G, De Benedetti F, Bracci-Laudiero L. NGF and its receptors in the regulation of inflammatory response. *Int J Mol Sci*. 2017;18:1028.

30. van den Borne SW, van de Schans VA, Strzelecka AE, et al. Mouse strain determines the outcome of wound healing after myocardial infarction. *Cardiovasc Res*. 2009;84:273–282.

31. Davies AM. Neurotrophins: more to NGF than just survival. *Curr Biol*. 2000;10:374–376.

32. Patel TD, Jackman A, Rice FL, Kucera J, Snider WD. Development of sensory neurons in the absence of NGF/TrkA signaling in vivo. *Neuron*. 2000;25:345–357.

33. Caporali A, Sala-Newby GB, Meloni M, et al. Identification of the prosurvival activity of nerve growth factor on cardiac myocytes. *Cell Death Differ*. 2008;15:299–311.

34. Meloni M, Caporali A, Graiani G, et al. Nerve growth factor promotes cardiac repair following myocardial infarction. *Circ Res*. 2010;106:1275–1284.

35. Jiang W, Ji M. Receptor tyrosine kinases in PI3K signaling: the therapeutic targets in cancer. *Semin Cancer Biol*. 2019;59:3–22.

36. Cocco E, Scaltriti M, Drilon A. NTRK fusion-positive cancers and TRK inhibitor therapy. *Nat Rev Clin Oncol*. 2018;15:731–747.

37. Drilon A, Laetsch TW, Kummar S, et al. Efficacy of larotrectinib in TRK fusion-positive cancers in adults and children. *N Engl J Med*. 2018;378:731–739.

38. Martinez-Jimenez F, Movasati A, Brunner SR, et al. Pan-cancer whole-genome comparison of primary and metastatic solid tumours. *Nature*. 2023;618:333–341.

KEY WORDS heart failure, mammary tumor, myocardial infarction, nerve growth factor, TRKA, tumor progression

APPENDIX For expanded Methods and References sections as well as supplemental figures and tables, please see the online version of this paper.